Taylor & Francis
Taylor & Francis Group

BRIEF REPORT

Effect of truncation on TRPM7 channel activity

Zhuqing Xie ⓘ and Nashat Abumaria ⓘ

State Key Laboratory of Medical Neurobiology and MOE Frontiers Center for Brain Science, Institutes of Brain Science, Fudan University, Shanghai, China

ABSTRACT

Transient receptor potential melastatin-like 7 (TRPM7) is a key player in various physiological and pathological processes. TRPM7 channel activity is regulated by different factors. The effects of cleavage of different domains on channel activity remain unknown. Here, we constructed several TRPM7 clones and explored the effects of truncating the mouse TRPM7 at different locations on the ion channel activity in two cell lines. We compared the clones' activity with the full-length TRPM7 and the native TRPM7 in transfected and untransfected cells. We also expressed fluorescently tagged truncated clones to examine their protein stability and membrane targeting. We found that truncating the kinase domain induced reduction in TRPM7 channel activity. Further truncations beyond the kinase (serine/threonine rich domain and/or coiled-coil domain) did not result in further reductions in channel activity. Two truncated clones lacking the TRP domain or the melastatin homology domain had a completely nonfunctional channel apparently due to disruption of protein stability. We identified the shortest structure of TRPM7 with measurable channel activity. We found that the truncated TRPM7 containing only S5 and S6 domains retained some channel activity. Adding the TRP domain to the S5-S6 resulted in a significant increase in channel activity. Finally, our analysis showed that TRPM7 outward currents are more sensitive to truncations than inward currents. Our data provide insights on the effects of truncating TRPM7 at different locations on the channel functions, highlighting the importance of different domains in impacting channel activity, protein stability, and/or membrane targeting.

Introduction

Transient receptor potential melastatin-like 7 (TRPM7) is a chanzyme having an ion channel part with a kinase domain in its C-terminal [1,2]. TRPM7 contains a highly conserved N-terminal, six transmembrane helixes (S1-S6), a highly conserved TRP domain, a coiled-coil domain, a serine/threonine rich domain, and an α-kinase domain [3]. TRPM7 emerges as a key player in various physiological and pathological processes [4,5]. Studies suggest that TRPM7 might be truncated on the C-/N-terminals during certain physiological and/or pathological processes leaving behind a truncated ion channel on the cell membrane [6–9]. The activity of the ion channel after such truncations remains unknown.

TRPM7 channel activity is regulated by several factors including intracellular Mg^{2+}, ATP [10–12],

ATP-activated kinase domain [2], cAMP/PKA signaling pathway [13], acidic pH [14], and phosphatidylinositol 4,5 bisphosphate (PIP_2) [15]. Truncating TRPM7 at different locations also results in changes in the channel activity. For example, truncated human TRPM7 without the kinase domain (amino acids 1–1569) exhibits only one-tenth of the full-length channel activity when expressed in HEK cells [16]. Similarly, truncated mouse TRPM7 without the kinase domain show no significant channel activity in CHO cells (amino acids 1–1599) [17] and in embryonic stem cells (amino acids 1–1537) [18]. In contrast, mouse TRPM7 cleaved at D1510 (without the kinase domain and the serine/threonine rich domain) exhibited significantly high channel activity when expressed in CHO cells [6]. Two truncated zebrafish TRPM7 (amino acids 1–1478 without kinase

CONTACT Nashat Abumaria ✉ Abumaria@fudan.edu.cn

domain and 1–1258 without the kinase and the serine/threonine rich domain) have similar activity to that of wild-type TRPM7 in HEK T-REX cells [19]. Meanwhile, when the zebrafish TRPM7 is truncated at the coiled-coil domain (amino acids 1–1178) the channel activity becomes even greater than that of the wild type [19]. Therefore, truncating TRPM7 at different locations results in different effects on the channel activity. However, in these studies, experiments were performed using TRPM7 clones from different species, TRPM7 was expressed in different cell lines, and the recording conditions were not identical. It remains unclear whether the reported different activities stem from the location of truncation or due to other methodological reasons.

Here, we constructed a series of mouse TRPM7 clones truncated at different locations, expressed these truncations in HEK and CHO cells, and examined the channel activity (inward and outward currents) of each truncation. Furthermore, we identified the shortest structure of TRPM7 that can retain ion channel activity.

Materials and methods

Molecular biology

For expression in mammalian cells, full-length TRPM7 and truncated TRPM7 were cloned into the pcDNA3.1 vector (Invitrogen, USA) and subsequently verified by double-strand DNA sequencing. Full-length TRPM7 and truncated TRPM7 (amino acids sequence: 1–1596, 1–1510, 1–1299, 1–1160, 1–1100, 756–1863, 990–1863, 990–1160, and 990–1100) clones were generated from mouse TRPM7 (Gene bank ID: NM_021450.2). Primers for constructing various clones of truncated TRPM7 are shown in Table 1.

Cell culture and transfection

Human embryonic kidney (HEK) cells were cultured in Dulbecco's modified Eagle's medium (DMEM, Gibco, USA) containing 10% fetal bovine serum (FBS, Gibco, USA). Chinese hamster ovary (CHO) cells were grown in DMEM/F12 supplemented with 10% FBS. Cells (~60% confluence, 25 flasks) were transiently transfected by 3.6 µg cDNAs carrying either TRPM7 (or other truncated mutations of TRPM7) or 0.4 µg EGFP cDNAs using Lipofectamine 3000 reagent (Thermo Fisher Scientific, USA). All cells were kept in a humidified incubator with 5% CO_2 at 37°C. Electrophysiological recordings were conducted 18–24 h after transfection.

Electrophysiological techniques

Whole-cell patch-clamp recordings were performed at room temperature using EPC-10 amplifier and Patch Master Software (HEKA, Germany). Currents were digitized at 10 kHz and low-pass filtered at 2.0 kHz. Pipettes with

Table 1. PCR primers of the full-length and truncated TRPM7 clones.

Gene		Sequence	Product, bp
mTRPM7	Forward	5′-cttggtaccgagctcggatccgccaccatgtcccagaaatcctggatag-3′	5589
	Reverse	5′-gttcgaatgggtgacctcgagctataacatcagacgaacagaatttgttgc-3′	
1–1596	Forward	5′-cttggtaccgagctcggatccgccaccatgtcccagaaatcctggatag-3′	4788
	Reverse	5′-aacgggccctctagactcgagctagctgttattcagtatactgggag-3′	
1–1510	Forward	5′-cttggtaccgagctcggatccgccaccatgtcccagaaatcctggatag-3′	4530
	Reverse	5′-aacgggccctctagactcgagctaatcgacttctggagagtcttc-3′	
1–1299	Forward	5′-cttggtaccgagctcggatccgccaccatgtcccagaaatcctggatag-3′	3897
	Reverse	5′-gttcgaatgggtgacctcgagctaggaactcagtgtgtttacagcac-3′	
1–1160	Forward	5′-cttggtaccgagctcggatccgccaccatgtcccagaaatcctggatag-3′	3480
	Reverse	5′-gttcgaatgggtgacctcgagctaaagttttggcccatcggaagtc-3′	
1–1100	Forward	5′-cttggtaccgagctcggatccgccaccatgtcccagaaatcctggatag-3′	3300
	Reverse	5′-gttcgaatgggtgacctcgagctaatatacattattgaaaaatgcgataaggag-3′	
756–1863	Forward	5′-cttggtaccgagctcggatccgccaccatgaattcctggtataaggtcatattaagc-3′	3321
	Reverse	5′-gttcgaatgggtgacctcgagctataacatcagacgaacagaatttgttgc-3′	
990–1863	Forward	5′-cttggtaccgagctcggatccgccaccatggtaatgatgattggaaaaatggtggcc-3′	2619
	Reverse	5′-gttcgaatgggtgacctcgagctataacatcagacgaacagaatttgttgc-3′	
990–1160	Forward	5′-cttggtaccgagctcggatccgccaccatggtaatgatgattggaaaaatggtggcc-3′	510
	Reverse	5′-gttcgaatgggtgacctcgagctaaagttttggcccatcggaagtc-3′	
990–1100	Forward	5′-cttggtaccgagctcggatccgccaccatggtaatgatgattggaaaaatggtggcc-3′	330
	Reverse	5′-gttcgaatgggtgacctcgagctaatatacattattgaaaaatgcgataaggag-3′	

an electrode resistance between 2 and 4 MΩ were prepared from borosilicate glass capillaries (World Precision Instruments, USA). The Mg^{2+}-free pipette solution contained (in mM): 145 CsCl, 8 NaCl, 10 HEPES, and 10 EGTA (pH 7.2 adjusted with CsOH). The bath solution contained (in mM): 140 NaCl, 5 KCl, 2 $CaCl_2$, 20 HEPES, and 10 glucose (pH 7.4 adjusted with NaOH). TRPM7 currents were recorded during repetitive injections of 300 ms voltage ramps from−100 to +100 mV repeated every 5 s at a holding potential of 0 mV. The presented TRPM7 channel currents at +100 and/or −100 mV were obtained when the currents reached a steady state (it stops changing for at least 30 ramps).

Immunocytochemistry

HEK cells transfected with full-length TRPM7-m-cherry and all truncations cDNAs were washed in PBS and fixed in PBS containing 4% paraformaldehyde for 30 min at room temperature. The cells were permeabilized in 0.2% TritonX-100 in PBS for 10 min and then incubated in blocking solution (5% goat serum for 120 min). Cells were incubated with Alexa Fluor™ 647 phalloidin (1:50, #A22287, Invitrogen, USA) for 20 min at room temperature. After washing, the cells were sealed by using VECTASHIELD® Antifade Mounting Medium with DAPI (#H-1200, VECTOR, USA). Cells were imaged by using 60× NA 1.42 oil immersion lens at zooms 1 and 3 mounted on OLYMPUS FLUOVIEW FV3000 confocal microscope at image resolution of 1024 × 1024.

Drugs

NS8593 was obtained from Sigma-Aldrich (St. Louis, USA), dissolved in DMSO to prepare a 20 mM solution and was stored at−20°C until use. NS8593 (10 μM) was used to block and/or identify TRPM7 currents. The blocker was added when no changes in current at +100 mV were observed for up to 10 s (after two successive ramps with similar currents). The concentration of DMSO in bath solution did not exceed 0.05%.

Data analysis

All patch clamp data were processed using Clampfit 11.1 (Molecular Device, USA) and then analyzed using GraphPad Prism 7 (GraphPad Software, USA). The minimum sample size was determined by using G*Power software (V3.1.9.4). We used the following parameters: α = 0.05, power = 0.8, and the effect size that is calculated by the mean and SD of the two groups of data. Sample number was matching or larger than the calculated minimum sample size. GraphPad Prism was used for normality, variance homogeneity, and other statistical analyses. Shapiro–Wilk test was used to test for normality test. The current density (pA/pF) was measured from the ratio of peak current amplitude (pA) to the cell membrane (pF). The data were presented as means ± SEM and the significance estimated by using unpaired two-tailed Student's t-tests (or Mann–Whitney test) or one-way ANOVA. P-value <0.05 was considered significantly different.

Results

Effect of truncating the C-terminal at different locations on TRPM7 channel activity

Starting from N-terminal, TRPM7 chanzyme contains melastatin homology domain (MH domain), six transmembrane helixes (S1-S6), a highly conserved TRP domain, a coiled-coil domain, a serine/threonine rich domain, and an α-kinase domain (Figure 1(a)). TRPM7 produces prominent outward currents at positive potentials from +50 to +100 mV and small inward currents at negative potentials between−100 and −40 mV [20,21]. Under our experimental conditions, the outward current (at +100 mV) is carried by the major internal monovalent cation Cs+, while the inward current (at −100 mV) is carried exclusively by the permeable divalent ion Ca^{2+} [1,2,22]. We first recorded the endogenous TRPM7-like current in untransfected HEK and CHO cells. The current densities of endogenous TRPM7 were 4.85 ± 0.55 pA/pF at +100 mV and−3.15 ± 0.34 pA/pF at −100 mV in HEK cells (Figure 1(b)). The current densities of endogenous TRPM7 were 9.99 ± 1.95 pA/pF (outward current we measured it at +100 mV) and−4.04 ± 0.34 pA/pF (inward current we
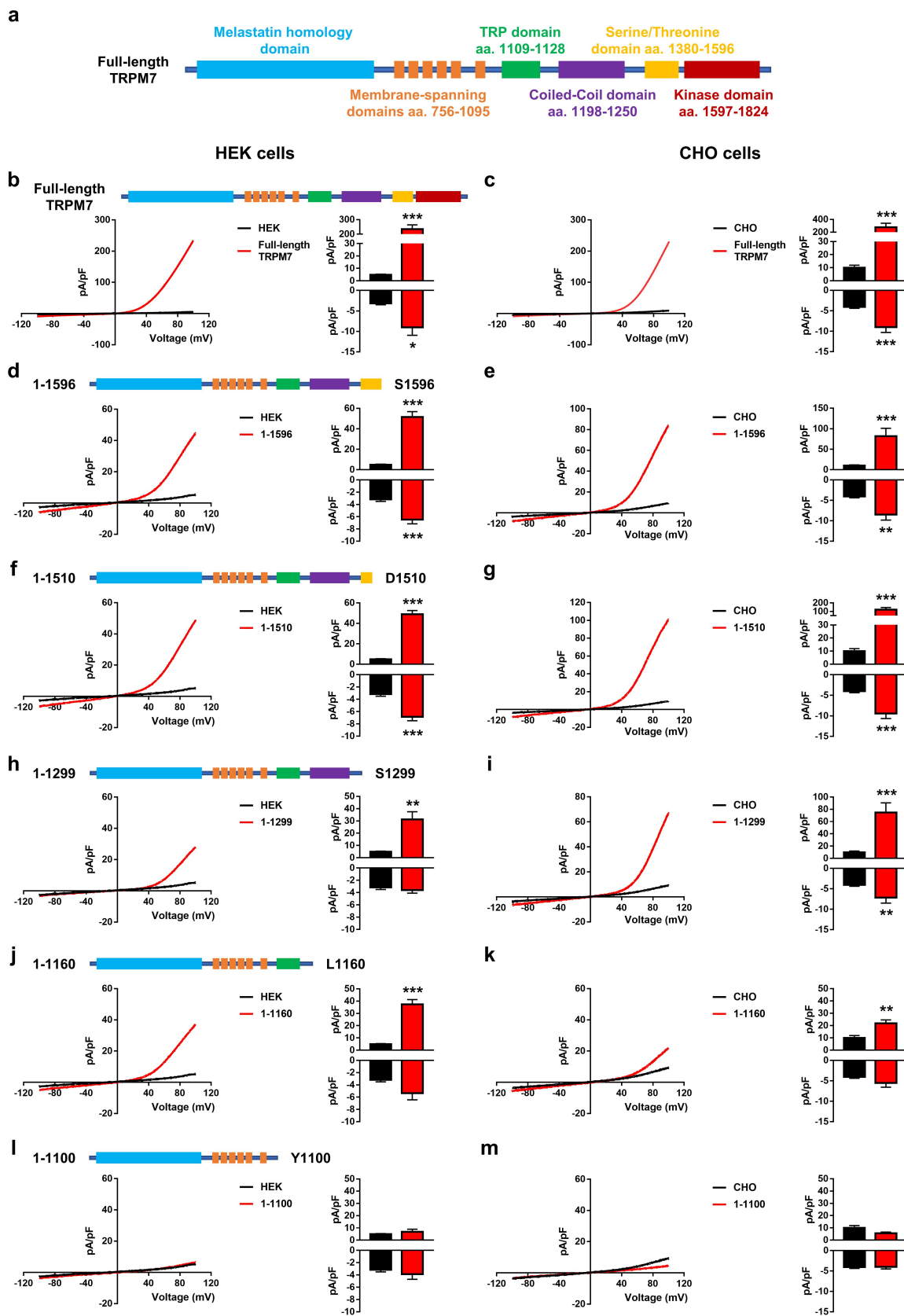
Figure 1. Effect of truncating the C-terminal at different locations on TRPM7 channel activity. (a) Schematic structure of TRPM7 channel. (b). Top panel: Schematic structure of full-length TRPM7. Left panel: Representative current-voltage relationships of untransfected HEK cells (black, $n = 7$) and full-length TRPM7 (red, $n = 7$) expressed in HEK cells. Right panel: Bar graphs of outward currents (+100 mV) and inward currents (−100 mV) gained from untransfected HEK cells (black) and full-length TRPM7 (red). (c). Left

measured it at −100 mV) in CHO cells (Figure 1(c)), which were similar to magnitudes reported by previous studies [2,23]. The recorded TRPM7-like currents can be blocked by NS8593 in untransfected HEK (Figure S1(a)) and CHO (Figure S1(b)) cells, indicating that the recorded currents are likely to be mediated by endogenous TRPM7 activity.

We then examined TRPM7 channel activity after we overexpressed the full-length TRPM7 in HEK and CHO cells. We found that overexpression of full-length TRPM7 resulted in a significant increase in the outward current density by 48.37 ± 6.07 folds (unpaired t test, $t_{(12)} = 7.800$, $p < 0.001$) and in the inward current density by 2.86 ± 0.62 folds (Unpaired t test, $t_{(12)} = 2.972$, $p = 0.012$) in comparison with untransfected HEK cells (Figure 1(b)). In CHO cells, following the overexpression of full-length TRPM7, the outward current density was significantly increased by 27.86 ± 6.15 folds (Unpaired t test, $t_{(14)} = 5.771$, $p < 0.001$); the inward current was increased by 2.23 ± 0.32 folds (Unpaired t test, $t_{(14)} = 4.640$, $p < 0.001$) in comparison with untransfected cells (Figure 1(c)). The recorded currents of the cells transfected with full-length TRPM7 can be blocked by NS8593, indicating that the recorded currents were mediated by TRPM7 activity (Figure S1(c)).

We then examined the effect of truncating different domains on the C-terminal side on the channel activity of TRPM7. A truncated TRPM7 lacking the kinase domain (amino acids 1–1596) exhibited outward current density of 51.64 ± 5.13 pA/pF (10.65 ± 1.10 folds compared with untransfected cells, unpaired t test, $t_{(19)} = 6.351$, $p < 0.001$). The inward current density was−6.48 ± 0.71 pA/pF (2.05 ± 0.22 folds compared with untransfected cells, Mann–Whitney test, $U = 5$, $p < 0.001$) in HEK cells (Figure 1(d)). In CHO cells, we found that the outward current density was 82.07 ± 18.93 pA/pF (8.21 ± 1.89 folds compared

with untransfected cells, Mann–Whitney test, $U = 0$, $p < 0.001$) and the inward current was−8.47 ± 1.36 pA/pF (2.10 ± 0.34 folds compared with untransfected cells, unpaired t test, $t_{(17)} = 3.324$, $p = 0.004$, Figure 1(e)). A shorter TRPM7 clone truncated within the serine/threonine rich domain (amino acids 1–1510) exhibited outward current density up to 48.97 ± 3.53 pA/pF (10.10 ± 0.76 folds compared with untransfected cells, unpaired t test, $t_{(18)} = 9.108$, $p < 0.001$) and inward current density of−6.86 ± 0.65 pA/pF (2.17 ± 0.21 folds compared with untransfected cells, unpaired t test, $t_{(18)} = 4.119$, $p < 0.001$) in HEK cells (Figure 1(f)). In CHO cells, the current densities of the 1–1510 truncated TRPM7 were 119.64 ± 25.91 pA/pF (11.97 ± 2.59 folds compared with untransfected cells, unpaired t test, $t_{(17)} = 4.459$, $p < 0.001$) and−9.43 ± 1.24 pA/pF (2.33 ± 0.31 folds compared with untransfected cells, Unpaired t test, $t_{(17)} = 4.405$, $p < 0.001$, Figure 1(g)). A truncated TRPM7 clone with complete loss of the kinase and the serine/threonine rich domains (amino acids 1–1299) had outward current density of 31.25 ± 6.27 pA/pF (6.44 ± 1.29 folds compared with untransfected cells, unpaired t test, $t_{(14)} = 3.678$, $p = 0.003$) and inward current density of−3.58 ± 0.51 pA/pF (1.13 ± 0.16 folds compared with untransfected cells, Mann–Whitney test, $U = 27$, $p = 0.681$) in HEK cells (Figure 1(h)). The truncated TRPM7 1–1299 in CHO cells also exhibited high outward current (74.63 ± 15.84 pA/pF, 7.49 ± 1.59 folds compared with untransfected cells, unpaired t test, $t_{(13)} = 5.809$, $p < 0.001$) and inward current (−7.17 ± 1.33 pA/pF, 1.78 ± 0.33 folds compared with untransfected cells, unpaired t test, $t_{(13)} = 3.038$, $p < 0.010$, Figure 1(i)). TRPM7 truncated at the coiled-coil domain (amino acids 1–1160) had outward current density of 37.43 ± 3.82 pA/pF (7.72 ± 0.79 folds compared with untransfected cells, unpaired t test, $t_{(13)} = 7.871$, $p < 0.001$) and inward

panel: Representative current-voltage relationships of untransfected CHO cells (black, $n = 10$) and full-length TRPM7 (red, $n = 6$) expressed in CHO cells. Right panel: Bar graphs of outward currents (+100 mV) and inward currents (−100 mV) gained from untransfected CHO cells (black) and full-length TRPM7 (red). Detection of truncated clones 1–1596 (d, $n = 14$), 1–1510 (f, $n = 13$), 1–1299 (h, $n = 9$), 1–1160 (j, $n = 8$), and 1–1100 (l, $n = 7$) were performed and analyzed similarly to (b) in HEK cells. Detection of truncated clones 1–1596 (e, $n = 14$), 1–1510 (g, $n = 9$), 1–1299 (i, $n = 5$), 1–1160 (k, $n = 5$), and 1–1100 (m, $n = 9$) were performed and analyzed similarly to (c) in CHO cells. Data are analyzed by two-tailed unpaired Student's t-tests or Mann–Whitney test and presented as mean ± SEM, *p < 0.05, **p < 0.01, ***p < 0.001.

current density of -5.35 ± 0.51 pA/pF $(1.70 \pm 0.35$ folds compared with untransfected cells, unpaired t test, $t_{(13)} = 1.180$, $p = 0.093$) in HEK cells (Figure 1(j)). In CHO cells, the current densities were 21.79 ± 2.85 pA/pF $(2.18 \pm 0.29$ folds compared with untransfected cells, unpaired t test, $t_{(13)} = 3.454$, $p = 0.004$) and -5.52 ± 1.04 pA/pF $(1.37 \pm 0.26$ folds compared with untransfected cells, unpaired t test, $t_{(13)} = 1.719$, $p = 0.109$, Figure 1(k)).

Therefore, loss of the kinase domain (1–1596), partial (1–1510) or complete (1–1299) loss of the serine/threonine rich domain, and/or complete loss of the coiled-coil domain (1–1160) did not completely abolish the channel activity as overexpression of these truncations induced TRPM7 currents that were significantly higher than that in untransfected HEK or CHO cells. However, all truncations (1–1596, 1–1510, 1–1299, and 1–1160) resulted in significant reductions in outward currents: 0.22 ± 0.02 folds (one way ANOVA: $F_{(5, 52)} = 54.620$, $p < 0.001$), 0.21 ± 0.02 folds (one way ANOVA: $F_{(5, 52)} = 54.620$, $p < 0.001$), 0.13 ± 0.03 folds (one way ANOVA: $F_{(5, 52)} = 54.620$, $p < 0.001$), and 0.16 ± 0.02 folds (one way ANOVA: $F_{(5, 52)} = 54.620$, $p < 0.001$; respectively) in comparison with full-length TRPM7 in HEK cells (Figure 2(a)). Similar results were obtained in CHO cells (1–1596: 0.29 ± 0.07 folds, one way ANOVA: $F_{(5, 37)} = 11.890$, $p < 0.001$; 1–1510: 0.43 ± 0.10 folds, one way ANOVA: $F_{(5, 37)} = 11.890$, $p < 0.001$; 1–1299: 0.27 ± 0.06 folds, one way ANOVA: $F_{(5, 37)} = 11.890$, $p < 0.001$; and 1–1160: 0.08 ± 0.01 folds, one way ANOVA: $F_{(5, 37)} = 11.890$, $p < 0.001$) (Figure 2(b)). Meanwhile, the inward current appeared to be resistant to these truncations. The inward currents of all truncations remained comparable to that observed in the full-length channel in both cell lines except for the 1–1299 truncated channel, which showed significant reductions in inward currents only in HEK cells (0.40 ± 0.06 folds, one way ANOVA: $F_{(5, 52)} = 4.075$, $p = 0.002$, Figure 2(a)). Expression of full-length or truncated clones of TRPM7 labeled with m-cherry in HEK cells revealed that the observed reductions in currents were likely to be mediated by reductions in channel activity, but not due to disruption of protein stability or cell membrane targeting (Figure 2(c)).

HEK cells transfected with TRPM7 clone truncated at the TRP domain (amino acids 1–1100) exhibited very low, if any, channel activity as its outward current density was 6.84 ± 2.07 pA/pF $(1.41 \pm 0.43$ folds compared with untransfected cells, unpaired t test, $t_{(12)} = 0.929$, $p = 0.371$) and inward current density -3.86 ± 0.84 pA/pF $(1.22 \pm 0.27$ folds compared with untransfected cells, unpaired t test, $t_{(12)} = 0.774$, $p = 0.454$, Figure 1(l)). In CHO cells, the current densities also did not differ between transfected and untransfected cells (outward: 5.53 ± 1.05 pA/pF, 0.55 ± 0.11 folds, unpaired t test, $t_{(17)} = 1.948$, $p = 0.068$; inward: -4.02 ± 0.50 pA/pF, 0.99 ± 0.12 folds, unpaired t test, $t_{(17)} = 0.042$, $p = 0.967$, Figure 1(m)). The channel activity of clone 1–1100 was significantly lower than that of full-length TRPM7 in HEK (outward current: 0.03 ± 0.01 folds, one way ANOVA: $F_{(5, 52)} = 54.620$, $p < 0.001$; inward current: 0.43 ± 0.09 folds, one way ANOVA: $F_{(5, 52)} = 4.075$, $p = 0.006$, Figure 2(a)) and CHO (outward current: 0.02 ± 0.01 folds, one way ANOVA: $F_{(5, 37)} = 11.890$, $p < 0.001$; inward current: 0.45 ± 0.06 folds, one way ANOVA: $F_{(5, 37)} = 3.701$, $p = 0.020$, Figure 2(b)) cells. Results suggested that the TRP domain is pivotal for TRPM7 channel activity. However, immunocytochemical analysis of the m-cherry tagged clone failed to detect fluorescent signal of the 1–1100 clone (Figure 2(c)) indicating that the loss of activity was most likely due to loss of protein stability, but not due to disruption of TRPM7 channel activity. Therefore, the TRP domain is pivotal for TRPM7 protein stability/expression.

Effect of truncating the N-terminal at different locations on TRPM7 channel activity

Next, we examined the channel activity after truncating TRPM7 on the N-terminal side. Truncation of the MH domain (amino acids 756–1863) resulted in complete loss of channel activity in HEK (outward current: 5.80 ± 1.28 pA/pF, 1.20 ± 0.26 folds compared with untransfected cells, unpaired t test, $t_{(15)} = 0.593$, $p = 0.562$; inward current: -3.22 ± 0.51 pA/pF, 1.02 ± 0.16 folds compared with untransfected cells, unpaired t test, $t_{(15)} = 0.095$, $p = 0.926$, Figure 3(a)) and CHO (outward current: 7.65 ± 1.19 pA/pF, 0.83 ± 0.13 folds
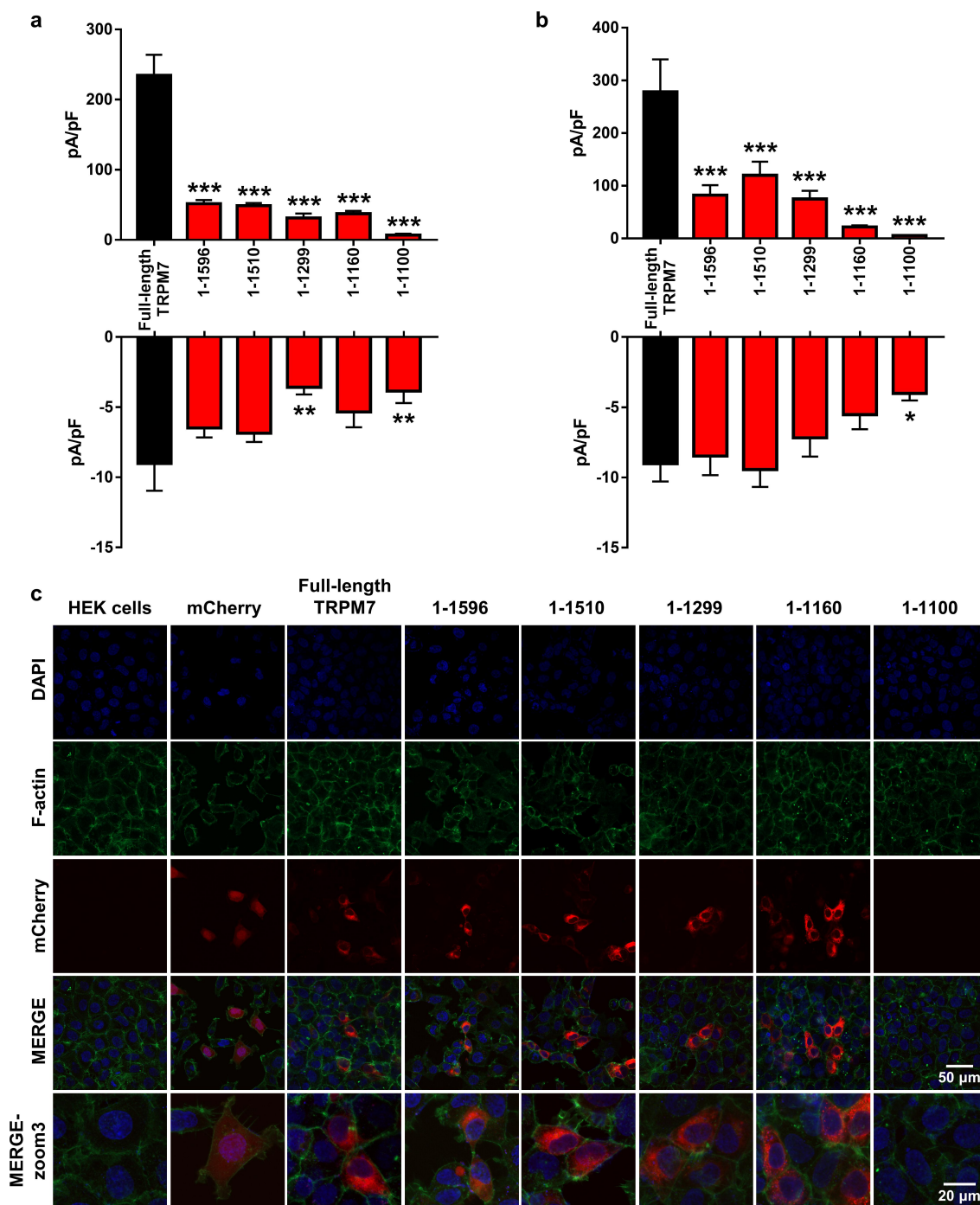
Figure 2. The outward and inward currents, and the expression pattern of different C-terminal truncations in comparison with full-length TRPM7. (a, b). Outward (top) and inward (bottom) current density of full-length TRPM7 (black) and truncations (1–1596, 1–1510, 1–1299, 1–1160, and 1–1100, red) in HEK (a) and CHO (b) cells. (c). Representative fluorescent images of HEK cells expressing full-length and the truncated TRPM7 clones labeled with m-cherry. The untransfected HEK cells were used as negative control. The TRPM7 clones labeled with m-cherry were in red. DAPI stained nuclei in blue. F-actin (Phalloidin staining, green) was used to indicate cell shape. Data are analyzed by one-way ANOVA and presented as mean ± SEM, *p < 0.05, **p < 0.01, ***p < 0.001.

compared with untransfected cells, unpaired t test, $t_{(15)} = 0.920$, $p = 0.372$; inward current: -5.46 ± 0.85 pA/pF, 1.35 ± 0.21 folds compared with untransfected cells, unpaired t test, $t_{(15)} = 1.744$, p

$= 0.102$, Figure 3(b)) cells. The channel activity of clone 756–1863 was significantly lower than that of full-length TRPM7 in HEK (outward current: 0.02 ± 0.01 folds, one way ANOVA: $F_{(4, \ 31)} =$
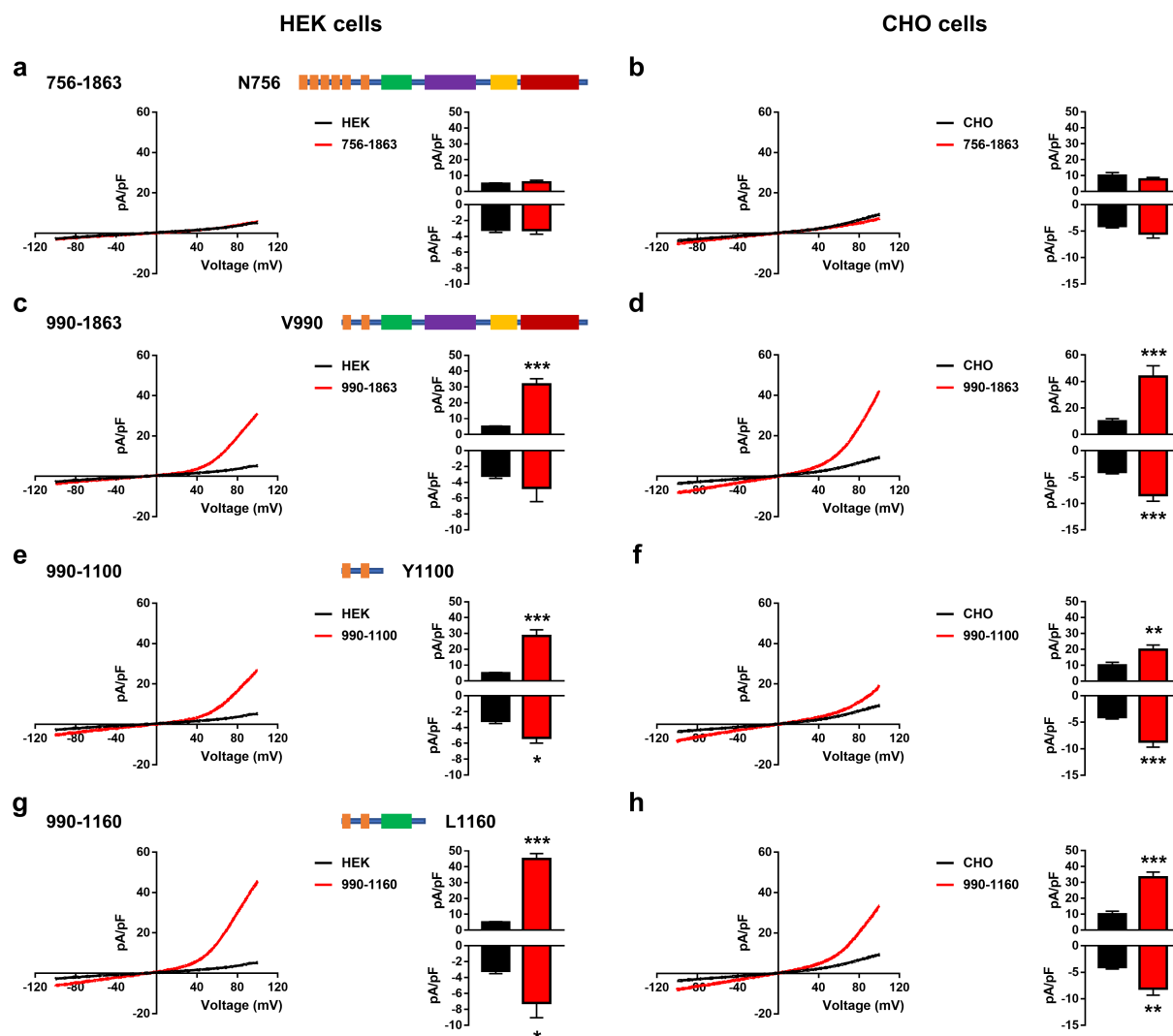
Figure 3. Effect of truncating the N-terminal at different locations on TRPM7 channel activity, and the smallest structure with channel activity. (a). Top panel: Schematic structure of truncated clone 756–1893. Left panel: Representative current-voltage relationships of untransfected HEK cells (black, $n = 7$) and truncated clone 756–1863 (red, $n = 10$) expressed in HEK cells. Right panel: Bar graphs of outward currents ($+100$ mV) and inward currents (-100 mV) gained from untransfected HEK cells (black) and truncated clone 756–1863 (red). (b). Left panel: Representative current-voltage relationships of untransfected CHO cells (black, $n = 10$) and truncated clone 756–1863 (red, $n = 7$) expressed in CHO cells. Right panel: Bar graphs of outward currents ($+100$ mV) and inward currents (-100 mV) gained from untransfected CHO cells (black) and truncated clone 756–1863 (red). Detection of truncated clones 990–1863 (c, $n = 8$), 990–1100 (e, $n = 6$), and 990–1160 (g, $n = 5$) were performed and analyzed similarly to (a) in HEK cells. Detection of truncated clones 990–1863 (d, $n = 6$), 990–1100 (f, $n = 7$), and 990–1160 (h, $n = 5$) were performed and analyzed similarly to (b) in CHO cells. Data are analyzed by two-tailed unpaired Student's t-tests or Mann–Whitney test and presented as mean $\pm$ SEM, *$p < 0.05$, **$p < 0.01$, ***$p < 0.001$.

52.100, $p < 0.001$; inward current: 0.36 ± 0.06 folds, one way ANOVA: $F_{(4, 31)} = 2.864$, $p = 0.014$, Figure 4(a)) and CHO (outward current: 0.03 ± 0.01 folds, one way ANOVA: $F_{(4, 26)} = 17.720$, $p < 0.001$, Figure 4(b)) cells. Results suggested that the MH domain is pivotal for TRPM7 channel activity. However, immunocytochemical analysis of the m-cherry tagged clone failed to detect

fluorescent signal of the 756–1863 clone (Figure 4(c)) indicating that the loss of activity was most likely due to loss of protein stability, but not due to disruption of TRPM7 channel activity. Therefore, the MH domain is pivotal for TRPM7 protein stability/expression.

In contrast, cells transfected with a shorter truncated TRPM7 without the MH domain and the
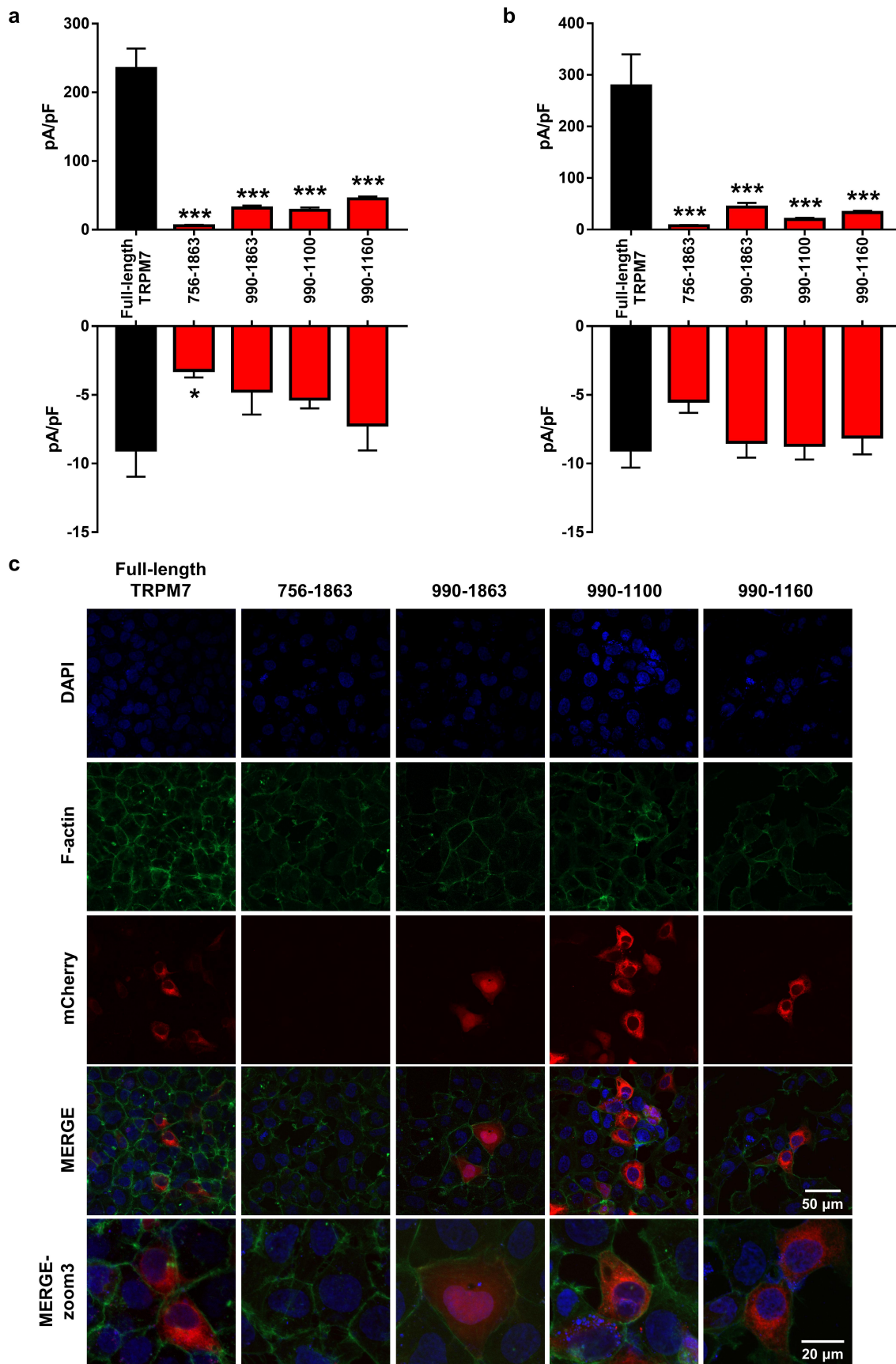
Figure 4. The outward and inward currents, and the expression pattern of different N-terminal truncations in comparison with full-length TRPM7. (a, b). Outward (top) and inward (bottom) current density of full-length TRPM7 (black) and truncations (756–1863,

transmembrane S1-S4 domains (amino acids 990–1863) exhibited higher currents than that in untransfected cells in HEK (outward current: 31.64 ± 3.61 pA/pF, 6.53 ± 0.74 folds, unpaired t test, $t_{(13)} = 6.854$, $p < 0.001$; inward current: -4.73 ± 1.70 pA/pF, 1.50 ± 0.54 folds, Mann–Whitney test, $U = 27$, $p = 0.955$, Figure 3(c)) and CHO (outward current: 43.69 ± 8.11 pA/pF, 4.37 ± 0.81 folds, unpaired t test, $t_{(14)} = 5.071$, $p < 0.001$; inward current: -8.45 ± 1.12 pA/pF, 2.09 ± 0.28 folds, unpaired t test, $t_{(14)} = 4.608$, $p < 0.001$, Figure 3(d)) cell lines. The channel activity of clone 990–1863 was significantly lower than that of full-length TRPM7 in HEK (outward current: 0.13 ± 0.02 folds, one way ANOVA: $F_{(4, 31)} = 52.100$, $p < 0.001$, Figure 4(a)) and CHO (outward current: 0.16 ± 0.03 folds, one way ANOVA: $F_{(4, 26)} = 17.720$, $p < 0.001$, Figure 4(b)) cells. However, examinations of m-cherry tagged clone by immunocytochemistry revealed that the clone was expressed but was not fully on the cell membrane (Figure 4(c)) suggesting that the observed reduction in activity was likely due to reductions in cell membrane targeting. Results also demonstrated that truncating the transmembrane domains S1-S4 recovered the inward current in comparison with the full-length TRPM7 (Figure 4(a, b)). Thus, truncating the S1-S4 reduced outward channel activity and impaired membrane targeting.

The shortest TRPM7 clone with channel activity

Finally, we explored the shortest structure of TRPM7 that is capable of exhibiting channel activity. The transmembrane domains S5 and S6 of the channel form the ion-permeable channel pore [24]. We constructed a truncated clone that only includes the pore forming domains (S5 to S6, amino acids 990–1100) and tested whether it is capable of exhibiting channel activity. We found that the outward current density was 28.47 ± 3.82 pA/pF (5.87 ± 0.79 folds compared with untransfected cells, unpaired t test, $t_{(11)} = 6.630$, $p < 0.001$)

and the inward current density was -5.31 ± 0.67 pA/PF (1.68 ± 0.21 folds compared with untransfected cells, unpaired t test, $t_{(11)} = 3.002$, $p = 0.012$) in HEK cells (Figure 3(e)). In CHO cells, the outward current density was 19.60 ± 2.89 pA/pF (1.99 ± 0.29 folds compared with untransfected cells, unpaired t test, $t_{(15)} = 2.956$, $p < 0.001$) and the inward current density was -8.67 ± 1.04 pA/pF (2.15 ± 0.26 folds compared with untransfected cells, unpaired t test, $t_{(15)} = 4.867$, $p < 0.001$, Figure 3(f)). Clone 990–1100 exhibited significantly lower channel activity in comparison with that of full-length TRPM7 in HEK (outward current: 0.12 ± 0.02 folds, one way ANOVA: $F_{(4, 31)} = 52.100$, $p < 0.001$, Figure 4(a)) and CHO (outward current: 0.07 ± 0.01 folds, one way ANOVA: $F_{(4, 26)} = 17.720$, $p < 0.001$, Figure 4(b)) cells. Results also demonstrated that inward current of 990–1100 was similar to that of full-length TRPM7 (Figure 4(a, b)).

We tested if inserting the TRP domain could help in enhancing the channel activity of the S5-S6 truncated TRPM7. We found that the TRP-containing short TRPM7 clone (amino acids 990–1160) exhibited significant channel activity. In HEK cells, the outward current density was 44.93 ± 3.42 pA/pF (9.27 ± 0.71 folds compared with untransfected cells, unpaired t test, $t_{(10)} = 13.760$, $p < 0.001$) and inward current density was -7.19 ± 1.85 pA/pF (2.28 ± 0.59 folds compared with untransfected cells, unpaired t test, $t_{(10)} = 2.540$, $p = 0.029$, Figure 3(g)). In CHO cells, the outward current density was 33.29 ± 3.19 pA/pF (3.33 ± 0.32 folds compared with untransfected cells, unpaired t test, $t_{(13)} = 6.560$, $p < 0.001$) and inward current density was -8.06 ± 1.26 pA/pF (2.00 ± 0.31 folds compared with untransfected cells, unpaired t test, $t_{(13)} = 4.060$, $p = 0.001$, Figure 3(h)). The clone 990–1160 had significantly lower channel activity in comparison with that of full-length TRPM7 in HEK (outward current: 0.19 ± 0.01 folds, one way ANOVA: $F_{(4, 31)} = 52.100$, $p < 0.001$, Figure 4(a)) and CHO (outward current: 0.12 ± 0.01 folds, one way ANOVA: $F_{(4, 26)} = $

990–1863, 990–1100, and 990–1160, red) in HEK (a) and CHO (b) cells. (c). Representative fluorescent images of HEK cells expressing full-length and the truncated TRPM7 clones labeled with m-cherry. The HEK cells transfected with full-length TRPM7 were used as control. The TRPM7 clones labeled with m-cherry were in red. DAPI stained nuclei in blue. F-actin (Phalloidin staining, green) was used to indicate cell shape. Data are analyzed by one-way ANOVA and presented as mean ± SEM, *p < 0.05, ***p < 0.001.

17.720, $p < 0.001$, Figure 4(b)) cells. Examinations of m-cherry tagged clones by immunocytochemistry revealed that these two clones were expressed and targeted on cell membrane in similar pattern to that of full-length TRPM7 (Figure 4(c)) suggesting that these truncations directly affect the channel activity.

Importantly, the 990–1160 clone displayed significantly higher outward current amplitude than that of the 990–1100 truncated channel in HEK (outward current: 1.58 ± 0.12 folds, unpaired t test, $t_{(9)} = 3.143$, $p = 0.012$; inward current: 1.35 ± 0.35 folds, unpaired t test, $t_{(9)} = 1.029$, $p = 0.331$, Figure S1(e)) and CHO (outward current: 1.67 ± 0.16 folds, unpaired t test, $t_{(10)} = 3.073$, $p = 0.012$; inward current: 0.93 ± 0.15 folds, unpaired t test, $t_{(10)} = 0.373$, $p = 0.717$, Figure S1(f)). Finally, this short and active truncated TRPM7 clone (990–1160) still can be blocked by the TRPM7 blocker NS8593 (Figure S1(d)). Thus, 990–1100 and 990–1160 clones could represent the shortest truncated TRPM7 structures with the strongest TRPM7 channel activity.

Discussion

In the current study, we found that truncating TRPM7 at different locations resulted in different effects on the ion channel activity. We also found that the TRP domain on the C-terminal side and the MH domain on the N-terminal side are pivotal for protein stability/expression not for the channel activity *per se*. Meanwhile, clone 990–1863 truncated after the S1-S4 domains, appeared to exhibit both impairment of channel activity and disruption of membrane targeting. Finally, we identified the truncated channel 990–1160 as the shortest structure of TRPM7 that retained relatively high ion channel activity and still can be inhibited by a classical TRPM7 blocker.

In the current study, cutting the kinase domain resulted in a reduction in TRPM7 channel activity, which is in line with previous studies [6,16,17]. The kinase domain was shown to regulate the ion channel activity by autophosphorylation [2,16,17]. Furthermore, nucleotides such as ATP bind to the kinase domain (their binding site is on the C-terminal of the kinase domain) resulting in activation of the kinase domain and regulation of

the ion channel activity [2]. Therefore, loss of the autophosphorylation as well as the magnesium-nucleotide binding site by truncating the kinase domain might explain the reductions in ion channel activity. Further truncations beyond the kinase (up to amino acid 1160) did not result in further reductions in channel activity. The serine/threonine rich domain and coiled-coil domain are known as the autophosphorylation sites that regulate the channel activity [25]. Apparently, loss of the autophosphorylation mechanism due to the absence of the kinase resulted in this lack of effects of truncating the serine/threonine rich domain and/or the coiled-coil domain on the channel activity.

The TRP domain, a highly conserved region among many TRP channels, is critical for subunit tetramerization and allosteric gating of the ion channel [26]. Mutations on TRP domain result in nonfunctional TRP ion channels [27]. The TRP domain might modulate ion channel activity by physically interacting with the S4-S5 linker of TRPV1 and TRPM7 [28–30] or the S6 domain of TRPM8 [31]. In some TRP channels such as TRPM6, TRPM7, TRPM5, and TRPM8, the TRP domain regulates their activity by binding to PIP_2 [27,32]. Our results demonstrate that truncating TRPM7 at the TRP domain resulted in loss of protein stability and hence the channel activity was not detected. On the other hand, the MH domain is known to be critical for channel trafficking and assembly [33]. Deletion of the MH domain in TRPM4 or TRPM6 results in reductions in channel activity [34,35]. Furthermore, structural studies showed that the TRP domain interacts with the MH domain to regulate TRP channel activity including TRPM7 [36]. Structural analysis of TRPM7 suggests that the C-terminal helix stretches forward to reach to the MH domain on the N-terminal bringing it closer to the TRP domain, resulting in signal transmission from the MH to the S6 domain which might control pore gating [30]. In line with the above-mentioned studies, our results support the notion that TRP and MH domains are pivotal for ion channel activity. Truncating one of these two domains was sufficient to generate a nonfunctional channel. However, our results suggest that the complete loss of the

channel activity might stem from loss of protein stability. Further experiments are required to elucidate how MH and/or TRP domains regulate the stability of TRPM7 protein, and how loss of S1-S4 might protect protein stability but disrupt membrane targeting.

Interestingly, the truncated TRPM7 clone lacking the TRP and MH domains (containing only S5 and S6, 990–1100 clone) showed relatively stable protein expression and high channel activity. Adding the TRP domain (990–1160 clone) resulted in further increases in the channel activity. Therefore, the 990–1100 and 990–1160 clones can be considered as the shortest structures of TRPM7 with relatively high and detectable channel activity.

In conclusion, physiological and/or pathological processes that might cleave TRPM7 at different domains will likely result in regulations of channel activity (namely outward current), protein stability, and cell membrane targeting.

Acknowledgments

Disclosure statement

No potential conflict of interest was reported by the author(s).

Funding

ORCID

Zhuqing Xie ⬥ http://orcid.org/0000-0003-2553-2604
Nashat Abumaria ⬥ http://orcid.org/0000-0002-6516-9590

Data availability statement

Data are contained within the article or Supplementary Materials.

Author contributions

N.A. conceived, designed, and supervised the project. Z. X. conducted all experiments and data analysis. N.A. and Z. X. wrote the manuscript.

References

[1] Nadler MJS, Hermosura MC, Inabe K, et al. LTRPC7 is a Mg·ATP-regulated divalent cation channel required for cell viability. Nature. 2001 May 31;411 (6837):590–595. doi:10.1038/35079092. PubMed PMID: 11385574.

[2] Runnels LW, Yue L, Clapham DE. TRP-PLIK, a bifunctional protein with kinase and ion channel activities. Science. 2001 Feb 9;291(5506):1043–1047. doi:10.1126/science.1058519. PubMed PMID: 11161216.

[3] Chubanov V, Mittermeier L, Gudermann T. TRPM7 reflected in cryo-emirror. Cell Calcium. 2018 Dec;76:129–131. doi:10.1016/j.ceca.2018.11.004. PubMed PMID: 30470536.

[4] Abumaria N, Li W, Clarkson AN. Role of the chanzyme TRPM7 in the nervous system in health and disease. Cell Mol Life Sci. 2019 Sep;76(17):3301–3310. doi:10.1007/s00018-019-03124-2. PubMed PMID: 31073743.

[5] Abumaria N, Li W, Liu Y. TRPM7 functions in non-neuronal and neuronal systems: perspectives on its role in the adult brain. Behav Brain Res. 2018 Mar 15;340:81–86. doi:10.1016/j.bbr.2016.08.038. PubMed PMID: 27555537.

[6] Desai BN, Krapivinsky G, Navarro B, et al. Cleavage of TRPM7 releases the kinase domain from the ion channel and regulates its participation in Fas-induced apoptosis. Dev Cell. 2012 Jun 12;22(6):1149–1162. doi:10.1016/j.devcel.2012.04.006. PubMed PMID: 22698280; PubMed Central PMCID: PMCPMC3397829.

[7] Landman N, Jeong SY, Shin SY, et al. Presenilin mutations linked to familial Alzheimer's disease cause an imbalance in phosphatidylinositol 4,5-bisphosphate metabolism. Proc Natl Acad Sci U S A. 2006 Dec 19;103(51):19524–19529. doi:10.1073/pnas.0604954103. PubMed PMID: 17158800; PubMed Central PMCID: PMC1748258. eng.

[8] Oh HG, Chun YS, Kim Y, et al. Modulation of transient receptor potential melastatin related 7 channel by presenilins. Dev Neurobiol. 2012 Jun;72(6):865–877. doi:10.1002/dneu.22001. PubMed PMID: 22102510; PubMed Central PMCID: PMCPMC3727165.

[9] Liu YQ, Chen C, Liu YL, et al. TRPM7 is required for normal synapse density, learning, and memory at different developmental stages. Cell Rep. 2018 Jun 19;23 (12):3480–3491. doi:10.1016/j.celrep.2018.05.069. PubMed PMID: WOS:000435818300007; English.

[10] Demeuse P, Penner R, Fleig A. TRPM7 channel is regulated by magnesium nucleotides via its kinase domain. J General Physiol. 2006 Apr;127(4):421–434. doi:10.1085/jgp.200509410. PubMed PMID: WOS:000236304000006; English.

[11] Nadler MJS, Hermosura MC, Inabe K, et al. LTRPC7 is a Mg center dot ATP-regulated divalent cation channel required for cell viability. Nature. 2001 May 31;411 (6837):590–595. doi:10.1038/35079092. PubMed PMID: WOS:000168982500053; English.

[12] Schmidt E, Narangoda C, Norenberg W, et al. Structural mechanism of TRPM7 channel regulation by intracellular magnesium. Cellular and Molecular Life Sciences. 2022 May;79(5):ARTN 225. doi:10.1007/s00018-022-04192-7. PubMed PMID: WOS:000779754300003; English.

[13] Takezawa R, Schmitz C, Demeuse P, et al. Receptor-mediated regulation of the TRPM7 channel through its endogenous protein kinase domain. Proc Natl Acad Sci USA. 2004 Apr 20;101(16):6009–6014. doi:10.1073/pnas.0307565101. PubMed PMID: WOS:000220978000061; English.

[14] Chokshi R, Matsushita M, Kozak JA. Detailed examination of Mg2+ and pH sensitivity of human TRPM7 channels. Am J Physiol Cell Physiol. 2012 Apr;302(7): C1004–1011. doi:10.1152/ajpcell.00422.2011. PubMed PMID: WOS:000302342700006; English.

[15] Runnels LW, Yue LX, Clapham DE. The TRPM7 channel is inactivated by PIP2 hydrolysis. Nat Cell Biol. 2002 May;4(5):329–336. doi:10.1038/ncb781. PubMed PMID: WOS:000175325100013; English.

[16] Schmitz C, Perraud AL, Johnson CO, et al. Regulation of vertebrate cellular Mg2+ Homeostasis by TRPM7. Cell. 2003 Jul 25;114(2):191–200. doi:10.1016/S0092-8674(03)00556-7. PubMed PMID: WOS:000184378700009; English.

[17] Matsushita M, Kozak JA, Shimizu Y, et al. Channel function is dissociated from the intrinsic kinase activity and autophosphorylation of TRPM7/ChaK1. J Biol Chem. 2005 May 27;280(21):20793–20803. doi:10.1074/jbc.M413671200. PubMed PMID: WOS:000229242000077; English.

[18] Ryazanova LV, Rondon LJ, Zierler S, et al. TRPM7 is essential for Mg2+ homeostasis in mammals. Nature Communications. 2010 Nov; 1: ARTN 109 doi:10.1038/ncomms1108. PubMed PMID: WOS:000288224800007; English.

[19] Jansen C, Sahni J, Suzuki S, et al. The coiled-coil domain of zebrafish TRPM7 regulates Mg center dot nucleotide sensitivity. Scientific Reports. 2016 Sep 15; 6. ARTN 33459. doi:10.1038/srep33459. PubMed PMID: WOS:000383169900001; English.

[20] Monteilh-Zoller MK, Hermosura MC, Nadler MJ, et al. TRPM7 provides an ion channel mechanism for cellular entry of trace metal ions. J Gen Physiol. 2003 Jan;121(1):49–60. doi:10.1085/jgp.20028740. PubMed PMID: 12508053; PubMed Central PMCID: PMCPMC2217320.

[21] Kim BJ, Jeon JH, Kim SJ, et al. Regulation of transient receptor potential melastatin 7 (TRPM7) currents by mitochondria. Mol Cells. 2007 Jun 30;23(3):363–369. PubMed PMID: 17646711.

[22] Gualdani R, Gailly P, Yuan JH, et al. A TRPM7 mutation linked to familial trigeminal neuralgia: omega current and hyperexcitability of trigeminal ganglion neurons. Proc Natl Acad Sci U S A. 2022 Sep 20;119 (38):e2119630119. doi:10.1073/pnas.2119630119. PubMed PMID: 36095216; PubMed Central PMCID: PMCPMC9499596.

[23] Kollewe A, Chubanov V, Tseung FT, et al. The molecular appearance of native TRPM7 channel complexes identified by high-resolution proteomics. Elife. 2021 Nov 12;10. doi:10.7554/eLife.68544. PubMed PMID: 34766907; PubMed Central PMCID: PMCPMC8616561.

[24] Yee NS, Kazi AA, Yee RK. Cellular and developmental biology of TRPM7 CHannel-Kinase: implicated roles in cancer. Cells. 2014 Jul 30;3(3):751–777. doi:10.3390/cells3030751. PubMed PMID: 25079291; PubMed Central PMCID: PMCPMC4197629.

[25] Cai N, Bai ZY, Nanda V, et al. Mass spectrometric analysis of trpm6 and trpm7 phosphorylation reveals regulatory mechanisms of the channel-Kinases. Scientific Reports. 2017 Feb 21;7: ARTN 42739. doi:10.1038/srep42739. PubMed PMID: WOS:000394709700001; English.

[26] Valente P, Fernandez-Carvajal A, Camprubi-Robles M, et al. Membrane-tethered peptides patterned after the TRP domain (TRPducins) selectively inhibit TRPV1 channel activity. FASEB J. 2011 May;25(5):1628–1640. doi:10.1096/fj.10-174433. PubMed PMID: 21307333.

[27] Xie J, Sun BN, Du JY, et al. Phosphatidylinositol 4,5-bisphosphate (PIP2) controls magnesium gate-keeper TRPM6 activity. Scientific Reports. 2011 Nov 9;1 ARTN 146doi:10.1038/srep00146. PubMed PMID: WOS:000300555700001; English.

[28] Liao M, Cao E, Julius D, et al. Structure of the TRPV1 ion channel determined by electron cryo-microscopy. Nature. 2013 Dec 5;504(7478):107–112. doi:10.1038/nature12822. PubMed PMID: 24305160; PubMed Central PMCID: PMCPMC4078027.

[29] Cao E, Liao M, Cheng Y, et al. TRPV1 structures in distinct conformations reveal activation mechanisms. Nature. 2013 Dec 5;504(7478):113–118. doi:10.1038/nature12823. PubMed PMID: 24305161; PubMed Central PMCID: PMCPMC4023639.

[30] Duan JJ, Li ZL, Li J, et al. Structure of the mammalian TRPM7, a magnesium channel required during embryonic development. Proc Natl Acad Sci USA. 2018 Aug 28;115(35):Eb201–210. doi:10.1073/pnas.1810719115. PubMed PMID: WOS:00044286160016; English.

[31] Taberner FJ, Lopez-Cordoba A, Fernandez-Ballester G, et al. The region adjacent to the C-end of the inner gate in transient receptor potential melastatin 8 (TRPM8) channels plays a central role in allosteric channel activation. J Biol Chem. 2014 Oct 10;289 (41):28579–28594. doi:10.1074/jbc.M114.577478. PubMed PMID: 25157108; PubMed Central PMCID: PMCPMC4192508.

[32] Rohacs T, Lopes CMB, Michailidis I, et al. Pi(4,5)P-2 regulates the activation and desensitization of TRPM8 channels through the TRP domain. Nat Neurosci. 2005 May;8(5):626–634. doi:10.1038/nn1451. PubMed PMID: WOS:000228895100023; English.

[33] Wehage E, Eisfeld J, Heiner I, et al. Activation of the cation channel long transient receptor potential channel 2 (LTRPC2) by hydrogen peroxide. A splice variant reveals a mode of activation independent of ADP-ribose. J Biol Chem. 2002 Jun 28;277(26):23150–23156. doi:10.1074/jbc. M112096200. PubMed PMID: 11960981.

[34] XZS X, Moebius F, Gill DL, et al. Regulation of melastatin, a TRP-related protein, through interaction with a cytoplasmic isoform. Proc Natl Acad Sci USA. 2001 Sep 11;98(19):10692–10697. doi:10.1073/pnas. 191360198. PubMed PMID: WOS:000170966800037; English.

[35] Chubanov V, Waldegger S, Mederos Y, et al. Disruption of TRPM6/TRPM7 complex formation by a mutation in the TRPM6 gene causes hypomagnesemia with secondary hypocalcemia. Proc Natl Acad Sci U S A. 2004 Mar 2;101(9):2894–2899. doi:10.1073/ pnas.0305252101. PubMed PMID: 14976260; PubMed Central PMCID: PMCPMC365716.

[36] Bousova K, Zouharova M, Herman P, et al. TRPM7 N-terminal region forms complexes with calcium binding proteins CaM and S100A1. Heliyon. 2021 Dec;7 (12):e08490. doi:10.1016/j.heliyon.2021.e08490. PubMed PMID: 34917797; PubMed Central PMCID: PMCPMC8645431.